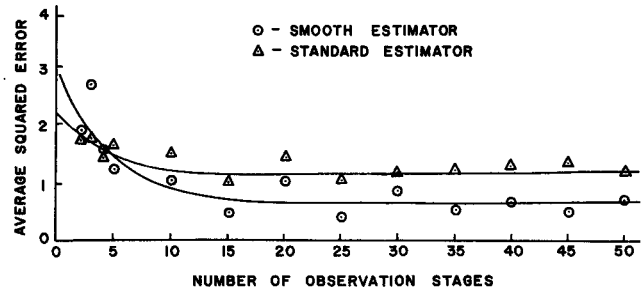

Fig. 1 Average squared error performance of the standard and smooth empirical Bayes estimators.

Performance Comparison

Monte Carlo simulation was employed to examine the average squared error loss incurred in using the estimator given by Eq. (9). For purposes of comparison the same dynamic system exemplified in Ref. 1 was again used here. The squared estimation errors $(\tilde{\theta}_n - \theta_n)^2$ were averaged for all five observation types over twenty-five replications for the standard estimator presented in Ref. 1 as well as for the estimator given here. The average squared errors are plotted in Fig. 1 at every fifth observation stage for both types of estimators. We observe that except for the first five stages, the smooth empirical Bayes estimator has an average squared error which is somewhat smaller than the standard empirical Bayes estimator. The same basic results were observed for numerous simulation runs using different sets of parameters. Thus, it appears that the estimator in Eq. (9) is somewhat superior in average squared error performance to the estimator in Ref. 1 and any gains should, in theory at least, be passed on to the Kalman state estimation procedure presented in Ref. 1.

References

[1] Martz, H. F. and Born, G. H., "Empirical Bayes Estimation of Observation Error Variances in Linear Systems," *AIAA Journal*, Vol. 9, No. 6, June 1971, pp. 1183–1187.

[2] Bennett, G. K. and Martz, H. F., "A Continuous Empirical Bayes Smoothing Technique," *Biometrika*, Vol. 59, No. 2, Aug. 1972, to be published.

[3] Martz, H. F. and Kamat, S. J., "Empirical Bayes State Estimation in Discrete Time Linear Systems," *AIAA Journal*, Vol. 9, No. 8, Aug. 1971, pp. 1654–1656.

[4] Parzen, E., "On Estimation of a Probability Density Function and Mode," *Annals of Mathematical Statistics*, Vol. 33, 1962, pp. 1065–1076.

[5] Abramowitz, M. and Stegun, I. A., *Handbook of Mathematical Functions*, National Burequ of Standards Applied Mathematics Series, 55, 1964.

[6] Gradshteyn, I. S. and Ryzhik, I. M., *Table of Integrals, Series, and Products*, Academic Press, New York, 1965.

Spreading of a Turbulent Disturbance

MICHAEL C. FISCHER*
NASA Langley Research Center, Hampton, Va.

Nomenclature

M = Mach number
x = distance along model wall, m
y = distance perpendicular to model surface, cm
z = coordinate in lateral direction, cm
δ = boundary layer thickness, cm
ϕ_{lateral} = disturbance lateral spreading angle, deg
ϕ_{spread} = disturbance total vertical spreading angle, deg
ϕ_{wall} = disturbance vertical spreading angle relative to wall, deg

Subscripts

e = boundary-layer edge conditions
0 = disturbance origin
tr = start of transition

Received January 17, 1972.

* Aerospace Engineer, Viscous Flows Section, Hypersonic Vehicles Division.

IN spite of the many experimental and theoretical studies dealing with the initial instabilities and subsequent transitional turbulent development of a boundary layer, very little is actually known about the initial disturbance growth behavior within the boundary layer. A recent paper[1] verified that the mean flow profiles in the outer portion of a hypersonic boundary layer ($M_e = 14$) are affected by transitional flow far upstream of the transition location indicated by wall heat-transfer measurements. Furthermore, an approximate spreading angle from the disturbance center (assumed to be near the critical layer) to the wall was shown to be shallow $\phi_{\text{wall}} \simeq 0.60°$. This Note extends the analysis of Ref. 1 to show the effect of local Mach number on both the turbulent disturbance spreading angle relative to the wall as well as lateral spreading.

To illustrate the effect of local Mach number on wall and lateral disturbance spreading angles, data from numerous investigations[1–21] were collected. With the exception of Ref. 1, and recent unpublished data obtained by the present author, all disturbance angles relative to the wall were determined from investigations where hot-wire contours[2,3] or hot-film surveys[4,7,13,20] of a "laminar" boundary layer were obtained. The spreading angle relative to the wall is herein defined as the angle formed by extending a straight line from the initial location where sizeable disturbances were first detected (known x and y values) in the laminar boundary layer down to the measured wall transition location. In our previous work (Ref. 1 and recent unpublished data) detailed spark schlierens showed protuberances at the outer edge of a laminar boundary layer far upstream of the wall transition location. The x location where these protuberances were first observed was taken as the initial disturbance origin, and a straight line from the critical layer height,[22] $y \simeq 0.90\,\delta$, extended down to the wall transition location was taken as the wall spreading angle.

Lateral disturbance spreading angles were obtained from investigations of: turbulent bursts,[5,16] reported observations of transverse contamination,[6,8] turbulent wedges formed behind isolated roughness specks,[10,18,21] and observed transitional oil flow[9,11,14,15,17] or other[19] visualization surface patterns both

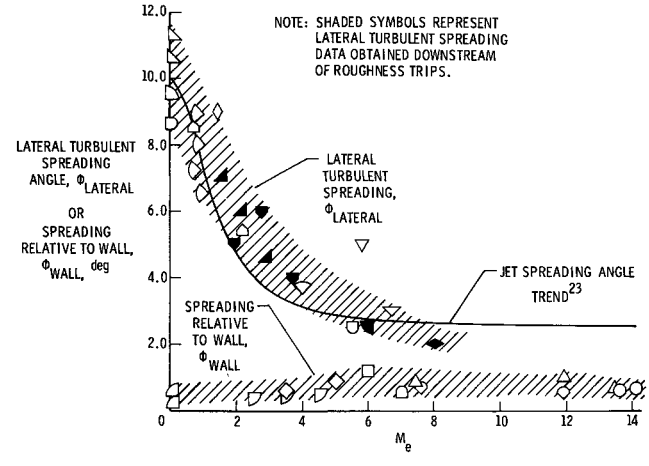

Fig. 1 Variation of turbulent spreading with local Mach number.

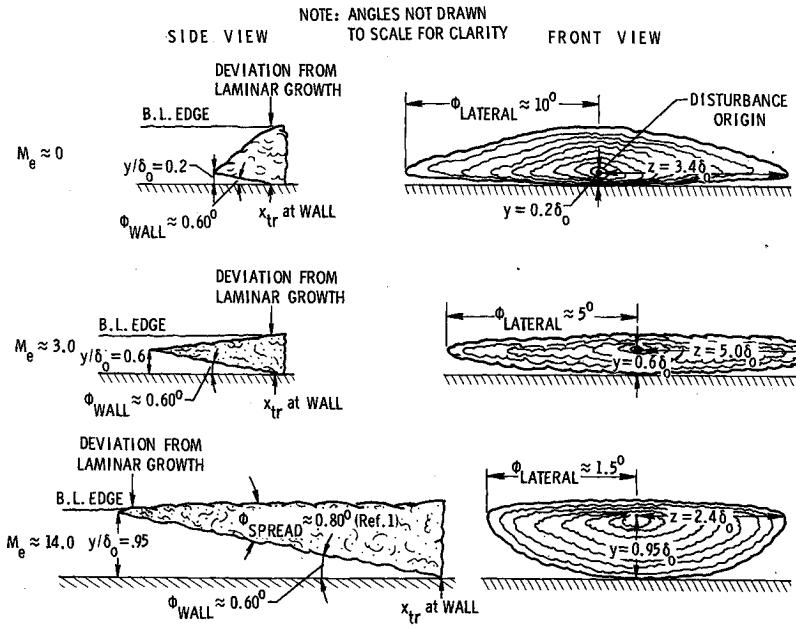

Fig. 2 Simplified cross sections of boundary-layer turbulence growth.

downstream of roughness trips and in untripped flow. In each case, the angle considered was the half-angle of the disturbance, assuming a symmetrical growth in the lateral direction. One may question whether the lateral spreading pattern downstream of a sizeable roughness trip,[9,11,15,17] which initially is a type of wake flow, is the same phenomena associated with the "free" spreading of a turbulent disturbance. The contention here is that once the flow downstream of a roughness trip becomes unstable (as verified from surface heat-transfer measurements, for instance), the turbulence spreading mechanism dominates. Further comment on this issue is presented in the following paragraph.

The variation of the wall and lateral disturbance spreading angles with local Mach number determined from the investigations of Refs. 1–21 is presented in Fig. 1. Note that the disturbance spreading angle relative to the wall seems to remain essentially invariant with Mach number while the lateral spreading angle decreases sharply with increasing Mach number up to about Mach 6. Lateral spreading data obtained downstream of roughness trips are shaded and indicate good agreement with other spreading data. This good agreement suggests that for both tripped and untripped flow, the lateral turbulent spreading characteristics are similar. Also, Fig. 1 shows a variation of turbulent jet spreading angle with Mach number, which is inversely proportional to the spreading parameter defined in Ref. 23. The lateral disturbance spreading angle data indicates general agreement with the jet spreading results implying that in the lateral dimension, turbulence in a boundary layer may develop essentially free of wall constraints (similar to a free shear layer).

Table 1 Summary of data used for determining lateral and wall spreading angles

SYMBOL	REFERENCE	METHOD FOR DETERMINING ANGLES	MODEL
○	Fischer and Weinstein[1]	Edge Disturbance	Cone, $\theta_c = 2.87°$
□	Staylor and Morrisette[2]	Hot-wire Contours	Flat Plate
◇	Potter and Whitfield[3]	Hot-wire Countours	Hollow Cylinder
△	Maddalon and Henderson[4]	Hot-film Surveys	Cones, $\theta_c = 2.87°, 5°, 10°$
◺	Schubauer and Klebanoff[5]	Turbulent Burst	Flat Plate
◻	Charters[6]	Transverse Contamination	Flat Plate
◻	LaGraff[7]	Hot-wire Surveys	Flat Plate
◇	Liepmann, et al.[8]	Transverse Contamination	Flat Plate
◿	Hicks and Harper[9]	Sublimation Pattern	Flat Plate.
⌂	Stalder and Slack[10]	Evaporization Pattern	Airfoil
◇	Stone and Cary[11]	Oil Flow Pattern	Flat Plate
▽	Korkegi[12]	Jet Trip Pattern	Flat Plate
◺	Klebanoff and Tidstrom[13]	Hot-wire Surveys	Flat Plate
▽	Wagner, et al.[14]	Oil Flow Pattern	Wedge
◻	Whitehead[15]	Oil Flow Pattern	Delta Wing
◻	Mitchner[16]	Turbulent Burst	Flat Plate
▽	Van Driest and McCauley[17]	Sublimation Pattern	Cone, $\theta_c = 5°$
◇	Loving and Katzoff[18]	Oil Film Pattern	Swept Wing
◻	Fischer[19]	Ablation Pattern	Cone, $\theta_c = 10°$
◻	Owen[20]	Hot-film Surveys	Flat Plate
◇	Hastings and Sawyer[21]	Sublimation Pattern	Flat Plate
◇	Fischer (Unpub.)	Edge Disturbance	Cone, $\theta_c = 5°, 10°$

It is interesting that the lateral and wall spreading angles (Fig. 1) exhibit only a moderate amount of scatter (except for Ref. 12) considering the wide variation in (and type of) tunnel disturbance environment, test model, wall temperature ratio, type of investigation, and condition of photographs, data, etc., available for determining these angles.

At this point, a comment is appropriate concerning a basic difference between the type of data used to determine the wall and lateral spreading angles. Wall spreading angles (except for Ref. 1 and recent unpublished data) were determined from hot wire or hot film studies, and thus these data represent a quasi-steady time average of many turbulent bursts. Conversely, the majority of the studies in which lateral spreading angles were measured dealt with isolated single bursts, turbulent wedges, or unstable flow downstream of a roughness trip. A direct comparison of the wall and lateral spreading angles to form a three-dimensional picture of turbulence, as done in the following section, may be accepted with some reservation because of these differences.

The insensitivity of wall spreading angle to local Mach number presents an interesting picture of the three-dimensional growth behavior of a turbulent disturbance. Since the location of the critical layer (assumed origin of disturbance) moves outward in the boundary layer with increasing Mach number,[3,22] the relatively constant wall spreading angle implies a greater "downstream lag" of wall boundary-layer transition as Mach number increases. This greater "downstream lag" with Mach number is further enhanced by the increased growth rate of the laminar boundary layer with Mach number and may be responsible for the observed steep increase of transition Reynolds number with increasing hypersonic Mach number. In fact, preliminary calcu

lations indicate that if the Reynolds number for transition is based on local Reynolds number and x at the disturbance origin, transition Reynolds number is weakly dependent on hypersonic Mach number for $M_e > 7$.

Together with the lateral spreading angle information, the wall spreading angle data makes it possible to construct simplified cross sections of three-dimensional turbulent disturbance growth behavior. Side and frontal views of these simplified cross sections are presented in Fig. 2 for three local Mach numbers; $M_e = 0$, $M_e = 3$, and $M_e = 14$. The varying nature of turbulence growth (based on Fig. 1) as a function of Mach number is evident. For the $M_e = 14$ case, the outer transitional growth which occurs far upstream of the wall transition location provides a plausible explanation for the observed increase[1,24] in experimental boundary-layer thicknesses (above the theoretical laminar value) upstream of transition. The visualization of turbulence growth and development presented herein may be of interest to the predictors who need to model transition in order to develop numerical techniques for transitional flow regions.

References

[1] Fischer, M. C. and Weinstein, L. M., "Cone Transitional Boundary-Layer Structure at $M_e = 14$," *AIAA Journal*, Vol. 10, No. 5, May 1972, pp. 699–701.

[2] Staylor, W. F. and Morrisette, E. L., "Use of Moderate-Length Hot-Wires to Survey a Hypersonic Boundary Layer," *AIAA Journal*, Vol. 5, No. 9, Sept. 1967, pp. 1698–1700.

[3] Potter, J. L. and Whitfield, J. D., "Effects of Slight Nose Bluntness and Roughness on Boundary-Layer Transition in Supersonic Flow," *Journal of Fluid Mechanics*, Vol. 12, 1962, pp. 501–535.

[4] Maddalon, D. V. and Henderson, A. Jr., "Boundary-Layer Transition on Sharp Cones at Hypersonic Mach Numbers," *AIAA Journal*, Vol. 6, No. 3, March 1968, pp. 424–431.

[5] Schubauer, G. B. and Klebanoff, P. S., "Contributions on the Mechanics of Boundary-Layer Transition," Rept. 1289, 1956, NACA.

[6] Charters, A. C. Jr., "Transition Between Laminar and Turbulent Flow by Transverse Contamination," TN 891, 1943, NACA.

[7] LaGraff, J. E., "Observations of Boundary-Layer Transition in Mach 7 Gun Tunnel with a Hot-Wire Anemometer," AIAA Paper 71-199, New York, 1971.

[8] Liepmann, H. W., Roshko, A., and Ohawan, S., "On the Reflection of Shock Waves from Boundary Layers," TN 2334, April 1951, NACA.

[9] Hicks, R. M. and Harper, W. R. Jr., "A Comparison of Spherical and Triangular Boundary Layer Trips on a Flat Plate at Supersonic Speeds," TM X-2146, Dec. 1970, NASA.

[10] Stalder, J. R. and Slack, E. G., "The Use of a Luminescent Lacquer for the Visual Indication of Boundary Layer Transition," TN-2263, Jan. 1951, NACA.

[11] Stone, D. R. and Cary, A. M. Jr., "Discrete Sonic Jets Used as Boundary Layer Trips at Mach Numbers of 6 and 8.5," Prospective TN D-(L-8215), 1972, NASA.

[12] Korkegi, R. H., "Transition Studies and Skin Friction Measurements on an Insulated Flat Plate at a Mach Number of 5.8," *Journal of the Aeronautical Sciences*, Vol. 23, No. 2, Feb. 1956, pp. 97–107, 192.

[13] Klebanoff, P. S. and Tidstrom, K. D., "Evolution of Amplified Waves Leading to Transition in a Boundary Layer with Zero Pressure Gradient," TN D-195, Sept. 1959, NASA.

[14] Wagner, R. D. Jr., Maddalon, D. V., and Weinstein, L. M., "Influence of Measured Free Stream Disturbances in Hypersonic Boundary Layer Transition," *AIAA Journal*, Vol. 8, No. 9, Sept. 1970, pp. 1664–1670.

[15] Whitehead, A. H. Jr., "Flow-Field and Drag Characteristics of Several Boundary Layer Tripping Elements in Hypersonic Flow," TN D-5454, Oct. 1969, NASA.

[16] Mitchner, M., "Propagation of Turbulence from an Instantaneous Point Disturbance," *Readers' Forum, Journal of the Aeronautical Sciences*, Vol. 21, No. 5, May 1954, pp. 350–351.

[17] Van Driest, E. R. and McCauley, W. D., "The Effect of Controlled Three-Dimensional Roughness on Boundary-Layer Transition at Supersonic Speeds," *Journal of the Aerospace Sciences*, April 1960, pp. 261–271, 303.

[18] Loving, D. L. and Katzoff, S., "The Fluorescent Oil Film Method and Other Techniques for Boundary Layer Flow Visualization," Memo 3-17-59 L, March 1959, NASA.

[19] Fischer, M. C., "An Experimental Investigation of Boundary Layer Transition on a 10° Half-Angle Cone at Mach 6.9," TN D-5766, April 1970, NASA.

[20] Owen, F. K., "Fluctuation and Transition Measurements in Compressible Boundary Layers," AIAA Paper 70-745, Los Angeles, Calif., 1970.

[21] Hastings, R. C. and Sawyer, W. G., "Turbulent Boundary Layers on a Large Flat Plate at $M = 4$," TR 70040, March 1970, Royal Aircraft Establishment, Bedford, England.

[22] Stainback, P. C., "Use of Rouse's Stability Parameter in Determining the Critical Layer Height of a Laminar Boundary Layer," *AIAA Journal*, Vol. 8, No. 1, Jan. 1970, pp. 173–175.

[23] Channapragada, R. S., "A Compressible Jet Spread Parameter for Mixing Zone Analysis," TM-14-63-U25, May 1963, United Technology Center.

[24] Fischer, M. C. and Maddalon, D. V., "Experimental Laminar, Transitional, and Turbulent Boundary Layer Profiles on a Wedge at Local Mach Number 6.5 and Comparisons with Theory," TN D-6462, Sept. 1971, NASA.

Reflection of Weak Shock Waves from Permeable Materials

G. S. BEAVERS* AND R. K. MATTA†

University of Minnesota, Minneapolis, Minn.

Introduction

In recent years considerable attention has been given to the use of permeable materials as sound attenuating devices, with particular interest concerned with the attenuating effects of the permeable material on the reflected and transmitted sound waves. Similarly, when a weak shock wave strikes a plane surface and is reflected, the strength of the reflected wave is lower when the reflecting surface is permeable than when the surface is impermeable. There appears, however, to be very little information available on the attenuation of shock waves reflected from permeable surfaces, although recently Cloutier and co-workers[1] have reported some observations on the attenuation of weak oblique shocks by porous surfaces. In this Note, we present some experimental observations which show the attenuating effects of three different permeable materials on the reflected shock strength. A simple analytical model is presented which consists essentially of the coupled problems of the reflection of a plane shock wave and the steady, compressible flow through a permeable material.

The flow configuration (Fig. 1) consists of a plug of permeable material positioned in a duct of constant cross-sectional shape. For this work, a permeable material is defined as a solid medium containing a large number of interconnected pores which are dispersed throughout the material in a random manner. The initial state is everywhere uniform, and the volume downstream of the permeable plug is very large, so that the pressure downstream of the material is assumed to remain constant. A plane shock wave strikes the front face of the permeable plug, and is reflected. The increased pressure thus formed at the front face of the plug creates a flow through the material. It is assumed that the material is sufficiently dense so that there is no transmitted

Received January 17, 1972; revision received February 23, 1972. This work was supported in part by the National Science Foundation under Grant GK 13303 and by the Department of Defense under Grant N00014-68-A-0141-0001 administered by the Office of Naval Research.

Index category: Shock Waves and Detonations.

* Associate Professor, Department of Aerospace Engineering and Mechanics. Member AIAA.

† Research Fellow, Department of Aerospace Engineering and Mechanics.